# Observation of Photon-Assisted Tunneling through a Quantum Dot

L. P. Kouwenhoven,* S. Jauhar, J. Orenstein, and P. L. McEuen
*Department of Physics, University of California at Berkeley, and Materials Science Division, Lawrence Berkeley Laboratory, Mail stop 2-200, Berkeley, California 94720*

Y. Nagamune, J. Motohisa,† and H. Sakaki
*Research Center for Advanced Science and Technology, University of Tokyo 4-6-1 Komaba, Meguro-ku, Tokyo 153, Japan*
(Received 25 July 1994)

We have measured dc transport through a GaAs/AlGaAs quantum dot in the presence of a microwave signal of frequency $f$. We find features related to the photon energy $hf$ whose positions in gate voltage are independent of the microwave power buy vary linearly with frequency. The measurements demonstrate photon-assisted tunneling in the mesoscopic regime. A comparison is made with a model that extends Coulomb blockade theory to include photon-assisted tunneling.

PACS numbers: 73.40.Gk, 73.20.Dx, 73.50.Mx, 73.50.Pz

An electron that tunnels in the presence of a potential $\tilde{V}\cos(2\pi ft)$ can exchange energy with this oscillating field. Such time-dependent tunneling can be divided into a classical regime ($hf \ll k_BT$) and a quantum regime ($hf \gg k_BT$). In the classical regime the energy exchange appears to be continuous, but in the quantum regime the discrete photon energy $hf$ becomes observable. Electrons can emit or absorb $n$ photons when they tunnel from an initial state $\varepsilon_i$ on one side of the barrier to a final state $\varepsilon_f$ on the opposite side, where $\varepsilon_f - \varepsilon_i = nhf$ and the integer $n \sim e\tilde{V}/hf$. Such *photon-assisted tunneling* (PAT) processes have been studied extensively in superconducting-insulating-superconducting tunnel junctions [1,2]. Recently, PAT has also been observed in superlattices irradiated by a free-electron laser [3].

In mesoscopic structures, high-frequency potentials are expected to yield new quantum effects due to the presence of phase coherence and/or charge quantization [4–6]. Theoretical work has focused mostly on noninteracting electron systems [4], but recently Coulomb blockade structures have also been examined [5,6]. Experiments with high-frequency signals in the quantum regime have been undertaken on quantum point contacts [7] and quantum dots [6]. The features observed by some of us in Ref. [6] were consistent with a model that combines PAT and Coulomb blockade theory. However, none of the mesoscopic experiments show the hallmark of PAT: transport features with a linear frequency dependence. In this Letter we demonstrate PAT through a quantum dot by the observation of microwave-induced features in the current whose positions are proportional to frequency and independent of power.

PAT through a quantum dot is illustrated in the schematic energy landscape in Fig. 1(a). The addition of an electron to the dot increases all levels by the charging energy $e^2/C$. Without radiation, Fig. 1(a) corresponds to the Coulomb blockade of transport [8]. When the conduction band bottom of the dot is varied by means of a gate voltage, transport is possible every time the lowest energy state for adding an electron to the dot aligns with the Fermi levels of the two reservoirs. The resulting *Coulomb oscillations* in the current versus gate voltage are a measure of the electron number in the dot; each period $\Delta V_g^{N\pm1}$ corresponds to a change of one electron. In the presence of radiation, inelastic single electron tunneling may occur due to the absorption or emission of photons. An example is depicted in Fig. 1(a); an electron can overcome the Coulomb gap and tunnel from the left reservoir into the dot by absorbing a photon. If the next tunnel event is from the dot to the right reservoir then this sequence contributes to the current. The condition for PAT involving a single photon is $|\varepsilon_i - \varepsilon_f| < hf$, where $\varepsilon_i$ is the highest possible initial state and $\varepsilon_f$ is the lowest possible final state. Experimentally, we an vary $|\varepsilon_i - \varepsilon_f|$ with a gate voltage and sweep through the single photon crossover $|\varepsilon_i - \varepsilon_f| = hf$. So, up to a distance $\Delta V_g^{hf}$ away from the center of a Coulomb oscillation we expect current induced by single photon-assisted tunneling, where $\Delta V_g^{hf}/\Delta V_g^{N\pm1} = hf/(e^2/C)$.

Our measurements are performed on a quantum dot defined by a combination of etching and metallic gates in a GaAs/AlGaAs heterostructure [see Fig. 1(b)] [9]. The two-dimensional electron gas (2DEG) has a mobility of about $10^6$ cm$^2$/V s and an electron density of $3.3 \times 10^{15}$ m$^{-2}$ after illumination at 4 K. The etching defines a narrow wire with an etched width of 0.8 $\mu$m (estimated conducting width of 0.4–0.5 $\mu$m) which widens into source and drain 2DEG regions. The five metallic gates can create five barriers (or four quantum dots) in series. For the experiment discussed in this Letter we use only gates 1 and 2 to define a single region of localized electrons. This quantum dot contains roughly 100 electrons and is weakly coupled via tunneling to the 2DEGs in the source and drain regions. In addition to applying dc voltages to gates 1 and 2, we can couple a microwave signal (0–40 GHz) to gate 1 via a capacitor

0031-9007/94/73(25)/3443(4)$06.00  

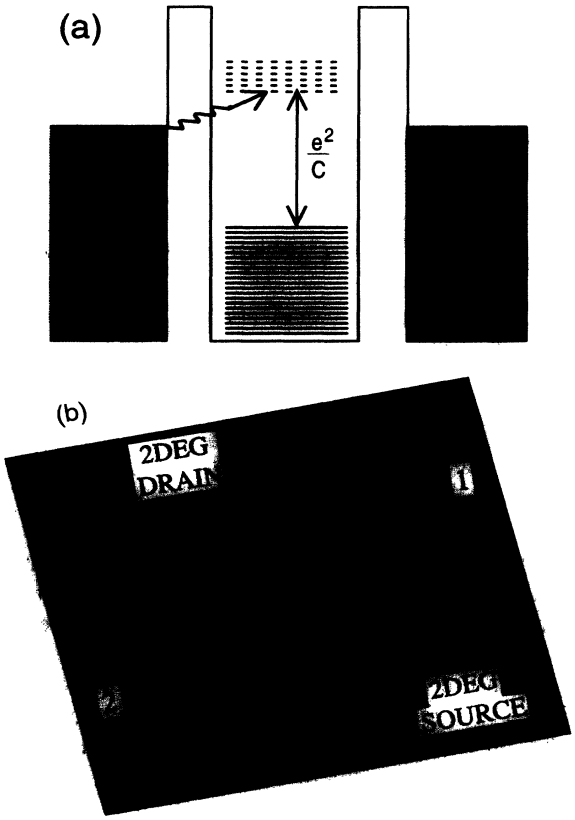


FIG. 1. (a) Energy diagram for a quantum dot in which the charging energy $e^2/C$ dominates. Solid lines in the dot are occupied levels while dotted lines are unoccupied. In the presence of microwaves an electron can overcome the Coulomb gap and tunnel into or out of the dot via absorption or emission of photons (the oscillating arrow is an example). (b) Atomic force microscope (AFM) picture of a narrow wire etched into the 2DEG of a GaAs/AlGaAs heterostructure. Five metallic gates cross the wire of which numbers 1 and 2 are used to define the quantum dot. The etched wire width is 0.8 $\mu$m and the distance between adjacent gates is 0.25 $\mu$m.

near the sample [10]. In this setup the microwave signal couples only to electrons in the vicinity of the quantum dot (within a region much smaller than a typical energy relaxation length of several $\mu$m).

We present measurements of the dc current $I$ versus the dc voltage $V_g$ on gate 1 at a small source-drain voltage $V_{sd} = 10$ $\mu$V. The voltage on gate 2 is fixed such that the tunnel conductance through this barrier is much smaller than $e^2/h$. The data are taken in a dilution refrigerator with a base temperature of 30 mK at a magnetic field of 3.35 T, which corresponds to a filling factor of 4 in the wide 2DEG regions. Similar results have been obtained at zero and other magnetic fields. The dashed curve in Fig. 2 shows a measurement of Coulomb oscillations without microwaves. From standard dc measurements [8] we obtain a charging energy $e^2/C = 0.33$ meV ($\pm 5\%$) and an effective electron temperature of approximately 100 mK. Finite $V_{sd}$ measurements did not

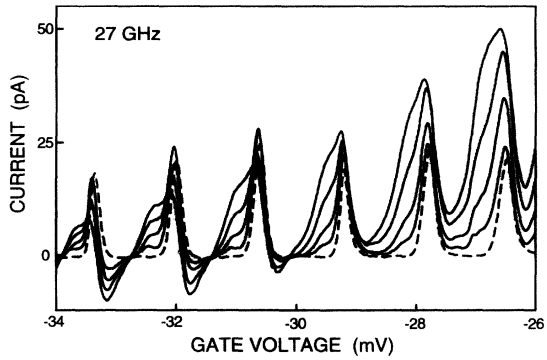


FIG. 2. Current versus gate voltage on gate 1 at $V_{sd} = 10$ $\mu$V. Dashed curve is without microwaves and solid curves are for increasing power in steps of 1 dBm at 27 GHz (higher induced current corresponds to higher power).

resolve a splitting of the single particle states implying that this splitting is smaller than a few times $k_BT$. The solid curves in Fig. 2 show Coulomb oscillations for different microwave powers at 27 GHz. The shape of the broadened Coulomb peaks gradually changes from peak to peak, but all the peaks contain a shoulder on the left side. The location of the shoulder is independent of the microwave power.

In Fig. 3(a) we show a similar set of measurements for three different frequencies. The shoulders are more pronounced at higher frequency, which illustrates the diminishing effect of thermal smearing (at 36 GHz, $hf = 0.15$ meV and $hf/kT = 17$ at 100 mK). Figure 3(b) shows the derivative of the current with respect to the gate voltage. Shoulders now appear as additional maxima, indicated by arrows, on the left side of each Coulomb oscillation. The location of each microwave-induced maximum is independent of power and shifts with frequency.

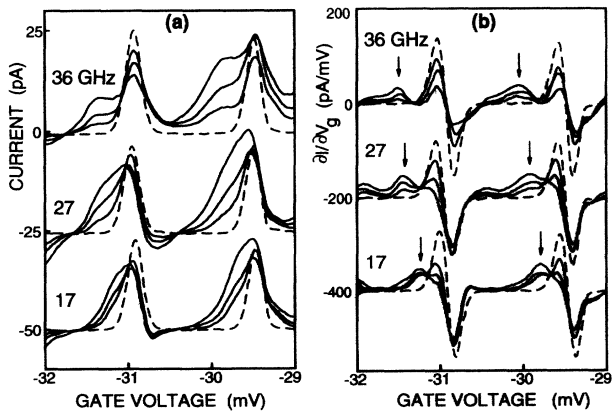


FIG. 3. (a) Current $I$ versus gate voltage $V_g$ on gate 1 at three different frequencies. Dashed curve is without microwaves and solid curves are for increasing power. (b) Derivatives $\partial I/\partial V_g$ of the curves shown in (a). Arrows indicate the photon-induced maxima. Different data sets are offset for clarity.

This frequency dependence is plotted in Fig. 4 for three different Coulomb peaks. The difference in gate voltage $\Delta V_g^{hf}$ is defined as the separation between the center of the peak without microwaves and the location of the microwave-induced maxima in the derivative curves. The plot of $\Delta V_g^{hf}$ converted into energy [8] versus the photon energy $hf$ shows that *the positions of the microwave-induced maxima vary linearly with frequency* between 9 GHz (the lowest frequency for which we could distinguish a microwave-induced maximum) and 36 GHz. This linear scaling indicates the PAT origin of the microwave-induced current. The solid line is a fit through the points corresponding to the peak centered at $V_g = -31$ mV. The dotted line is calculated and will be discussed below.

To calculate the effects of PAT through a quantum dot we use the ac model for Coulomb blockade devices presented in Ref. [6]. This ac model encompasses the Tien-Gordon theory [1] for PAT in a master equation from the "orthodox" Coulomb blockade theory. The microwave signal is modeled by two ac voltage amplitudes $\tilde{V}_S$ and $\tilde{V}_d$ across the course and drain junctions. Figure 5 shows a comparison between the measured photoresponse of a peak taken from Fig. 2 and a numerical solution of the ac model. The values for $e^2/C$, $T$, $f$, and $V_{sd}$ used in the calculation are taken from the experiment. The only adjustable parameters are the ac amplitudes $\tilde{V}_S$ and $\tilde{V}_d$. By assuming a small asymmetry in the ac coupling $\tilde{V}_d = 0.85\tilde{V}_S$ we obtain good agreement between the measured and calculated photoresponse [11,12]. The photon energy $hf$ on the theoretical gate voltage scale of Figs. 5(c) and 5(d) is indicated by the arrows. We find from such

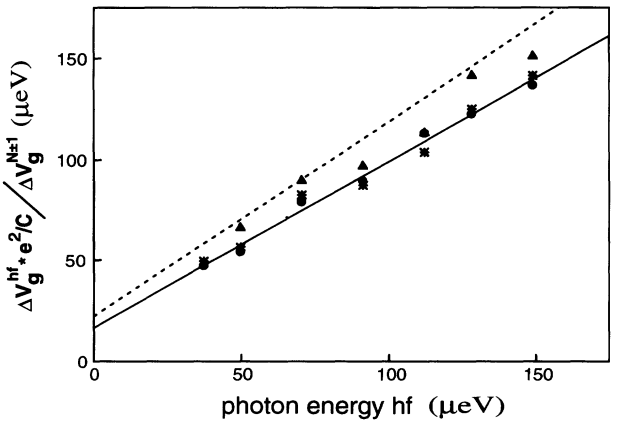


FIG. 4. Horizontal axis: Photon energy $hf$. Vertical axis: $\Delta V_g^{hf}$ is the difference in gate voltage between the location of the photon-induced maxima [i.e., arrows in Fig. 3(b)] and the zero crossing of the dashed curve (without microwaves). $\Delta V_g^{hf}$ is multiplied by the charging energy $e^2/C = 0.33$ meV and divided by the period $\Delta V_g^{N\pm1} = 1.4$ mV of the Coulomb oscillations to convert it into an energy. $\Delta V_g^{hf}$ is determined for three different Coulomb peaks (▲ is centered around $V_g = -36$ mV, ● around −31 mV, and ✻ around −28 mV) from 9 to 36 GHz. The solid line is a fit through the ● points. The dotted line is calculated (see text).

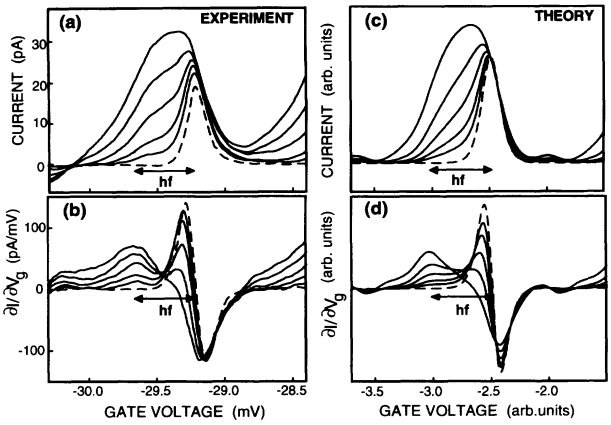


FIG. 5. Comparison between measurement and calculation. The parameters $e^2/C = 0.33$ meV, $f = 27$ GHz, $T = 100$ mK, and $V_{Sd} = 0.01$ mV in the calculation are taken from the experiment; the only adjustable parameters are the ac amplitudes $V_S$ and $V_d$. We have taken $V_d = 0.85V_S$, $V_S = 0$, 34, 47, 66, 92, and 129 $\mu$V [11]. The conversion of the gate voltage scale to energy in units of $hf$ is indicated by the arrows.

calculations that, independent of the precise parameter values, our definition of $\Delta V_g^{hf}$ is a good measure of $hf$.

With the same parameter values of Figs. 5(c) and 5(d) we obtain the dashed line in Fig. 4 for the calculated frequency dependence. Note that neither the experimental nor the theoretical line goes through the origin. The reason for this offset is that a difference in $\tilde{V}_S$ and $\tilde{V}_d$ can shift the center of a Coulomb oscillation in a similar fashion to a nonzero dc source-drain voltage. In contrast to this parameter-dependent offset, the slope is parameter independent and equal to 1 for the theoretical line in Fig. 4. The slope of the experimental dashed line is 0.87. This 13% discrepancy can be resolved by assuming a charging energy $e^2/C = 0.38$ meV instead of the experimental value 0.33 meV. Whether this means that the dc charging energy cannot directly be used to analyze high frequency experiments is unclear.

The data in Figs. 2 and 3 show a microwave-induced broadening mainly to the left of the Coulomb peaks. We found that this broadening can be shifted to the right or made almost symmetric by varying the magnetic field or frequency. Figure 2 shows that the photoresponse also gradually changes from peak to peak. Apparently, the asymmetry between $\tilde{V}_S$ and $\tilde{V}_d$ increases when $V_g$ is made more negative [negative current regions occur when $\tilde{V}_S - \tilde{V}_d$ exceeds the asymmetry set by $V_{sd}$ [6]]. Regardless of the precise shape of the broadening, however, we find that, for $f > 10$ GHz, the photon structure always scales with frequency and does not shift with power. The fact that the observed photoresponse depends on the dc gate voltage and the magnetic field implies that the relation between $\tilde{V}$ and $\tilde{V}_S, \tilde{V}_d$ depends on the local potential landscape. A detailed study of this relation would be interesting in connection with the recent theoretical work on mesoscopic admittances [13].

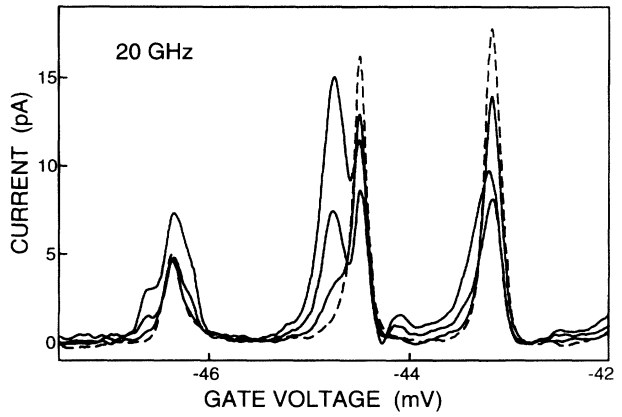


FIG. 6. Current versus dc gate voltage on gate 1. Dashed curve is without microwaves and solid curves are for increasing power at 20 GHz. The central peak shows a photoresponse that cannot be explained with the ac Coulomb blockade model of Ref. [6].

The comparison in Fig. 5 suggests that the photon structure is somewhat more pronounced in the measured data than in the calculation. This is often the case, especially at higher frequencies. Occasionally, very pronounced photon structure is observed; an example is shown in Fig. 6. The photoresponse of the peak in the middle contains a deep minimum between the central dashed peak and the photon-induced maximum. We find that the distance between the two maxima scales linearly with frequency, as expected for PAT. A lineshape with such a deep minimum, however, does not follow from the ac Coulomb blockade model and remains unexplained [14].

We would like to thank Dave Dixon, Michael Huang, Chandu Karadi, Kam Lau, Charlie Marcus, Yuli Nazarov, Nijs van der Vaart, and Keith Wald for discussions and experimental help. This work was supported by ONR, the Packard Foundation, the Sloan Foundation (P.L.M.), and the Royal Netherlands Academy of Arts and Sciences (L.P.K.)

*Present address: Department of Applied Physics, Delft University of Technology, P.O. Box 5046, 2600 GA Delft, The Netherlands.

†Present address: Research Center for Interface Quantum Electronics, Hokkaido University, North 13 West 8, Sapporo 060, Japan.

[1] P.K. Tien and J.R. Gordon, Phys. Rev. **129**, 647 (1963).

[2] See the review J.R. Tucker and M.J. Feldman, Rev. Mod. Phys. **57**, 1055 (1985).

[3] P.S.S. Guimarães, B.J. Keay, J.P. Kaminski, S.J. Allen, Jr., P.F. Hopkins, A.C. Gossard, L.T. Florez, and J.P. Harbison, Phys. Rev. Lett. **70**, 3792 (1993).

[4] M. Büttiker and R. Landauer, Phys. Rev. Lett. **49**, 1739 (1982); P. Johansson, Phys. Rev. B **41**, 9892 (1990); F. Hekking and Yu.V. Nazarov, Phys. Rev. B **44**, 9110 (1991); S. Feng and Q. Hu, Phys. Rev. B **48**, 5354 (1993); N.S. Wingreen, A.P. Jauho, and Y. Meir **48**, 8487 (1993); see also references therein.

[5] K. Flensberg *et al.*, Phys. Scr. **T42**, 189 (1992); K.K. Likharev and I.A. Devyatov, Physica (Amsterdam) **194–196B**, 1341 (1994); A. Hadicke and W. Krech, Physica (Amsterdam) **193B**, 256 (1994); C. Bruder and H. Schoeller, Phys. Rev. Lett. **72**, 1076 (1994).

[6] L.P. Kouwenhoven, S. Jauhar, K. McCormick, D. Dixon, P.L. McEuen, Yu.V. Nazarov, N.C. van der Vaart, and C.T. Foxon, Phys. Rev. B **50**, 2019 (1994).

[7] N.K. Patel *et al.*, *Proceedings of the 20th International Conference on the Physics of Semiconductors Thessaloniki, 1990*, edited by E.M. Anastassakis and J.D. Joannopoulos (1991) p. 2371; R.A. Wyss *et al.*, Appl. Phys. Lett. **63**, 1522 (1993); T.J.B.M. Janssen *et al.*, J. Phys. Condens. Matter **6**, L163 (1994); C. Karadi *et al.* (to be published).

[8] See for reviews of Coulomb blockade, D.V. Averin and K.K. Likharev, in *Mesoscopic Phenomena in Solids*, edited by B.L. Altshuler *et al.* (Elsevier, Amsterdam, 1991); *Single Charge Tunneling*, edited by H. Grabert and M.H. Devoret (Plenum, New York, 1992); See for a collection of quantum dot papers, *The Physics of Few-Electron Nanostructures*, L.J. Geerligs *et al.* [Physica (Amsterdam) **189B** (1993)].

[9] For fabrication details see, Y. Nagamune, H. Sakaki, L.P. Kouwenhoven, L.C. Mur, C.J.P.M. Harmans, J. Motohisa, and H. Noge, Appl. Phys. Lett. **64**, 2379 (1994).

[10] In a similar setup, single electron turnstiles and pumps have been measured but at much lower frequencies ($\sim$10 MHz for which $hf \ll k_BT$). For metallic systems see, L.J. Geerligs *et al.*, Phys. Rev. Lett. **64**, 2691 (1990); H. Pothier *et al.*, Physica (Amsterdam) **169B**, 573 (1991). For a quantum dot system see, L.P. Kouwenhoven *et al.*, Phys. Rev. Lett. **67**, 1626 (1991).

[11] The sequence of ac amplitudes in the calculation corresponds to increasing power in steps of 3 dBm, which is larger than the experimental steps of 1 dBm.

[12] The excellent agreement between theory and experiment suggests that the electron temperature does not rise significantly on applying microwaves. Other measurements to investigate this indicate that the electron temperature is less than 200 mK at the highest microwave powers.

[13] M. Büttiker, H. Thomas, and A. Prêtre, Z. Phys. B **94**, 133 (1994), and references therein.

[14] The assumptions of the model in Ref. [6] are (1) continuous single particle density of states, (2) a frequency $f$ much larger than the tunnel rates through the two barriers, (3) complete relaxation in the dot between tunnel events, and (4) ac amplitudes $\tilde{V}_d, \tilde{V}_S$ which are independent of dc gate voltage. We checked that the excitation spectrum is continuous and that there is no detectable phase separation of the Landau levels in the dot, which rule out a violation of condition (1). Moreover, the current level of order pA gives an average tunnel rate of 10–100 MHz so that condition (2) is also satisfied.

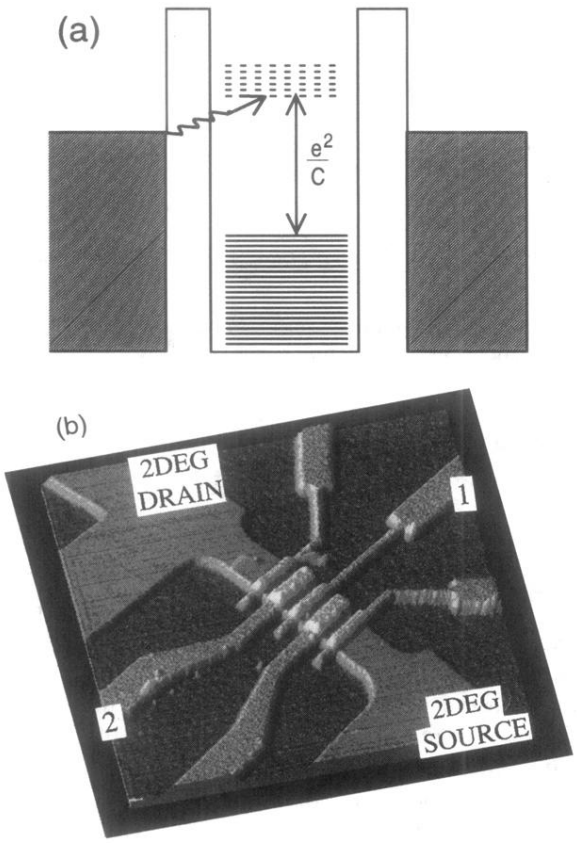


FIG. 1. (a) Energy diagram for a quantum dot in which the charging energy $e^2/C$ dominates. Solid lines in the dot are occupied levels while dotted lines are unoccupied. In the presence of microwaves an electron can overcome the Coulomb gap and tunnel into or out of the dot via absorption or emission of photons (the oscillating arrow is an example). (b) Atomic force microscope (AFM) picture of a narrow wire etched into the 2DEG of a GaAs/AlGaAs heterostructure. Five metallic gates cross the wire of which numbers 1 and 2 are used to define the quantum dot. The etched wire width is 0.8 $\mu$m and the distance between adjacent gates is 0.25 $\mu$m.